ASME Journal of Thermal Science and Engineering Applications
Online journal at:
https://asmedigitalcollection.asme.org/thermalscienceapplication

Zengxi Feng[1]
School of Building Services Science and Engineering,
Xi'an University of Architecture and Technology,
Xi'an 710055, China
e-mail: fzx4311@163.com

Wenjing Wang
School of Building Services Science and Engineering,
Xi'an University of Architecture and Technology,
Xi'an 710055, China
e-mail: 3306999844@qq.com

Xin He
School of Building Services Science and Engineering,
Xi'an University of Architecture and Technology,
Xi'an 710055, China
e-mail: 765070298@qq.com

Gangting Li
School of Building Services Science and Engineering,
Xi'an University of Architecture and Technology,
Xi'an 710055, China
e-mail: 1779591014@qq.com

Lutong Zhang
School of Building Services Science and Engineering,
Xi'an University of Architecture and Technology,
Xi'an 710055, China
e-mail: lutong0450@163.com

Weipeng Xiang
School of Building Services Science and Engineering,
Xi'an University of Architecture and Technology,
Xi'an 710055, China
e-mail: 1321823232@qq.com

Energy Saving Optimization of Chilled Water System Based on Improved Fruit Fly Optimization Algorithm

As the main energy consumption part of the central air-conditioning system, the energy saving of the chilled water system is particularly important. In this paper, an improved fruit fly optimization algorithm (IFOA) is used to optimize the operating parameters of the chilled water system to reduce the energy consumption of the chilled water system. In IFOA, the 3-D position coordinate is introduced to expand the search space of the algorithm, the variable-step strategy balances the global search ability and local search ability of the algorithm and helps a single fruit fly jump out of the local optimization through chaos mapping. In order to verify the optimization effect of IFOA on the chilled water system, the energy consumption model of the chilled water system is established. With the lowest total energy consumption of the system as the goal, the operating parameters such as the chilled water supply temperature and the speed ratio of the chilled water pump are optimized. The simulation results show that the energy-saving optimization method of a central air-conditioning chilled water system based on IFOA can make the average energy-saving rate of the system reach 7.9%. Compared with other optimization algorithms, the method has a better energy-saving effect and is more stable.
[DOI: 10.1115/1.4062359]

Keywords: chilled water system, fruit fly optimization algorithm, operating parameters, energy consumption model

1 Introduction

In the past decades, the rapid development of society has consumed a large amount of nonrenewable energy and emitted a large number of greenhouse gas into the atmosphere, leading to the rise of global temperature and the destruction of the earth's environment. In 2021, China's total energy consumption will reach 5.24 billion tons of standard coal, and carbon emissions will reach 11.47 billion tons, an increase of 5.15% and 1.5% respectively compared with 2020 [1]. There is still a big gap between China's total energy consumption and the main goal in the Opinions on Completely, Accurately and Comprehensively Implementing the New Development Concept to Do a Good Job in Carbon Peak and Carbon Neutralization issued by the CPC Central Committee and the State Council in 2021 [2]. Reducing social energy consumption is the key to achieving this goal. Studies indicate that building energy consumption accounts for 30–40% of total social energy consumption, and this value will continue to grow rapidly in the foreseeable future [3]. Therefore, energy efficiency studies of existing buildings are needed to achieve the goal of reducing building energy consumption.

Among the energy consumption of buildings, the energy consumption of the air-conditioning system occupies 40–60% or even more, which has great potential for energy saving [4]. The

[1]Corresponding author.

Manuscript received February 28, 2023; final manuscript received April 17, 2023; published online May 30, 2023. Assoc. Editor: Prabal Talukdar.

chilled water system is the most important energy consumption part of the air-conditioning system, and its operating energy consumption accounts for about 60% of the total energy consumption of the air-conditioning system [5,6]. Therefore, it is of great significance to conduct energy conservation research on the chilled water system. At present, researchers have conducted in-depth studies on the energy saving of central air-conditioning systems. Zhou et al. [7] proposed a PCA-ANN-based energy-saving control strategy to optimize the operation of central air-conditioning systems in subway stations, which can reduce air-conditioning operation energy consumption of subway stations by 10.5%. Yu et al. [8] proposed a variable frequency strategy for cooling tower fans and pumps, which can make the air-conditioning system operating energy consumption by 5.3%. Wijaya et al. [9] based on the EnergyPlus model, an optimization method combining an artificial neural network and genetic algorithm proposed to improve the efficiency of the air-conditioning system by dynamically optimizing the chilled water flow, thereby reducing the system energy consumption. Deng et al. [10] analyzed the influencing factors and characteristics of energy consumption of chilled water systems, proposed a system optimization method considering internal and external factors and their synergistic effects, and applied it to a high-rise office building and achieved considerable energy-saving effect. Yu et al. [11] proposed a distributed optimization based on a new distributed control structure and alternating direction multiplier method with regular terms algorithm to achieve a dynamic hydraulic balance of the chilled water system with minimum energy consumption. This method can save 28.54% of energy compared to the unfertilized operation strategy. Shi et al. [12] developed a control strategy for chilled water systems by establishing an approximate optimal performance diagram of the chilled water system equipment. The strategy has significant advantages over the two existing control strategies.

In recent years, swarm intelligence optimization algorithms have gradually emerged, which are widely used in various fields of engineering and natural sciences because of their simplicity of operation, ease of understanding, flexibility, superiority-seeking ability, and robustness. Du et al. [13] used a residual neural network to build an optimization model for chillers and introduced the gray wolf optimization algorithm to optimize the controllable variables of chillers to reduce the system energy consumption. Kusiak et al. [14] used a data mining algorithm to establish a nonlinear relationship between energy consumption and control parameters, modeled equipment such as pumps and fans, and solved it by a particle swarm optimization algorithm. The results showed that the operating energy consumption of the air-conditioning system was reduced by 7%. Jiao et al. [15] established a power consumption model for chilled water pumps and air-conditioning fans and proposed an energy-saving optimization method for air-conditioning systems based on an improved ant colony algorithm. The results showed that the method has a good energy-saving effect and has some advantages. Chen et al. [16] established the energy consumption models of chilled water pumps and fans and used a particle swarm optimization algorithm to establish an energy consumption optimization model as a way to reduce the energy consumption of the air-conditioning system. Ma et al. [17] used the recursive least squares method to identify the model parameters of air-conditioning system equipment and used a genetic algorithm for a central air-conditioning system energy consumption optimization using a genetic algorithm. The results showed that the method can save 0.73–2.55% of energy compared to the conventional scheme.

The fruit fly optimization algorithm (FOA) is a new intelligent optimization algorithm proposed by Dr. Wenchao Pan et al. [18] in Taiwan, China, based on the foraging behavior of the fruit fly population. Compared with other intelligent optimization algorithms, FOA is less computationally intensive, has a shorter running time, and has a better global foraging ability, but it is prone to premature maturation and other phenomena during operation, so it needs to be improved to obtain better foraging results. Yang et al. [19] introduced Gaussian variation and orthogonal learning into FOA to enhance the diversity of the population, which can effectively avoid premature convergence. Qi et al. [20] proposed a linear generation mechanism to uniformly generate candidate solutions, used a new variable-step method to balance the searchability of the algorithm in different periods, and verified the stability of the improved algorithm in three practical cases. Guo et al. [21] introduced two concepts of sensitivity and pheromone to improve the optimization strategy and location update method of FOA, which improved the diversity of the population as well as the local search ability. Chen et al. [22] introduced a random swimming mechanism in FOA to dynamically adjust the position of fruit fly populations and reduce the influence of the initial population position, thus enhancing the global optimization ability.

The aforementioned literature provides feasible directions for chilled water system optimization, but most of the studies on energy-saving optimization of chilled water systems are based on local optimization of individual equipment, lacking a systematic analysis of the synergistic operation between different equipment under actual cooling demand [23,24]. Therefore, in this paper, from the perspective of global energy saving of chilled water systems, the energy consumption model of chilled water system-related equipment is established, and the operating parameters of the system are optimized using the improved fruit fly optimization algorithm with controllable variables as optimization parameters to reduce the energy consumption of the system.

2 Research Methodology

In this paper, central air-conditioning system experimental equipment is used as the research object, which consists of a chiller, chilled water pump, cooling water pump, fan coil, cooling tower, and data acquisition system [25]. The data acquisition equipment: indoor and outdoor temperature and humidity sensors, wind speed sensors, multifunctional electric meters, electromagnetic flowmeters, and digital pressure gauges, which can collect the temperature, pressure, and flowrate of the system in real-time. The structure diagram of the experimental system is shown in Fig. 1.

The research framework of this paper is shown in Fig. 2, and the main steps are: (1) Obtain the real-time operational data of the experimental equipment of the central air-conditioning system through the data acquisition equipment. (2) Establish the equipment energy consumption model of the chilled water system. Identify the unknown parameters of the model using the least squares method in MATLAB, and verify the validity of the model. (3) With the minimum energy consumption of the chilled water system as the target and the controllable parameters as the decision variables, the system is optimized using IFOA to obtain the minimum energy consumption of the central air-conditioning chilled water system and its parameter settings under the condition of satisfying the system cooling demand.

3 Problem Description

A typical chilled water system consists of chillers, chilled water pumps, and other equipment. In the system, the chiller provides low-temperature chilled water for the system, and the chilled water flow is controlled by the chilled water pump to deliver it to the central air-conditioning terminal equipment for heat exchange with indoor air, and the chilled water returns to the chiller after completing the work, thus continuously circulating to achieve the indoor cold load demand. The working principle of the chilled water system is shown in Fig. 3.

3.1 Chiller Energy Modeling. The chiller is the most energy-consuming equipment in the chilled water system of central air-conditioning, and its main role is to transfer the heat of chilled water to cool water, to achieve the purpose of cooling. According to the chiller plant energy consumption model proposed by ASHRAE Handbook [26], the chiller plant energy consumption is

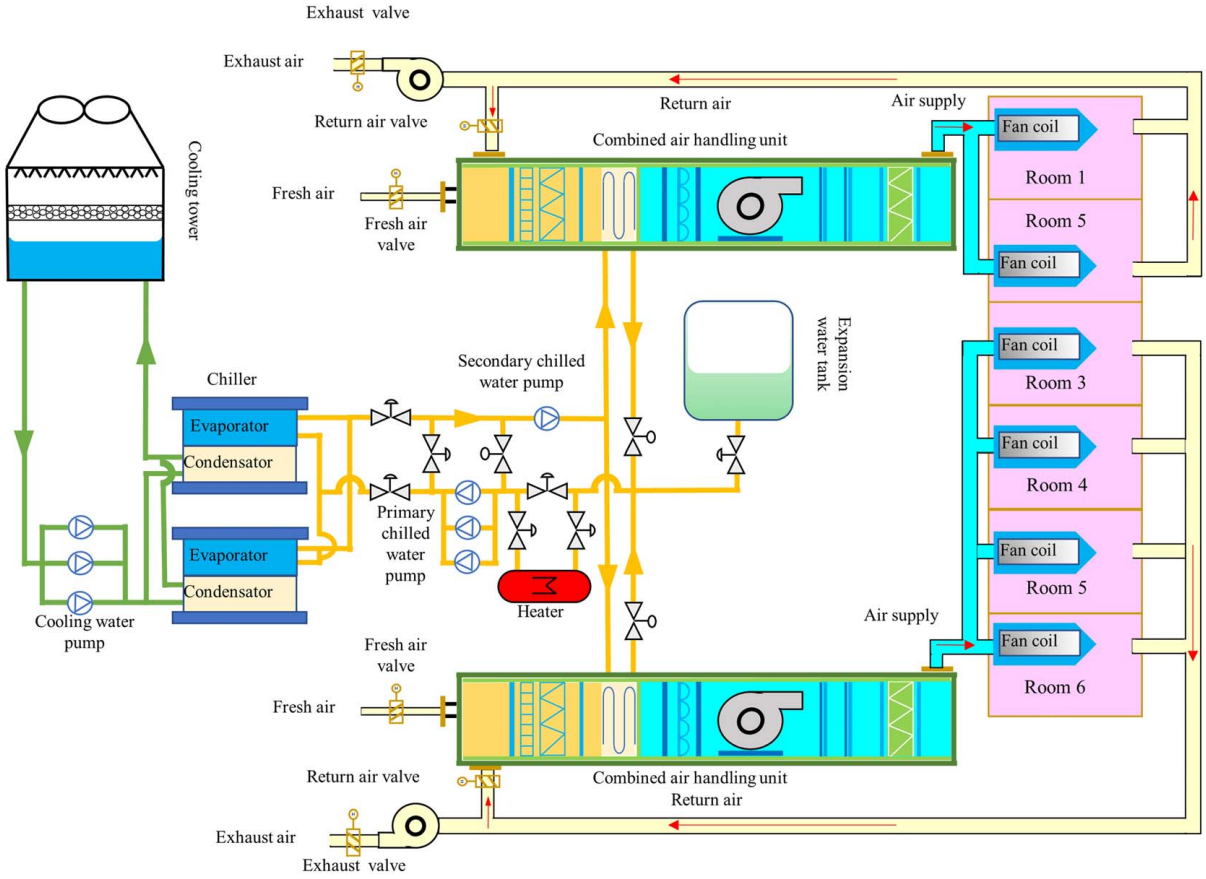

Fig. 1 Central air conditioning structure schematic

related to the unit load and evaporation temperature. The energy consumption model of the chiller unit can be expressed as follows:

$$P_{chiller} = a_1 + b_1 Q + c_1 Q^2 + d_1(T_{cws} - T_{chws}) + e_1(T_{cws} - T_{chws})^2 + f_1 Q(T_{cws} - T_{chws}) \quad (1)$$

where $P_{chiller}$ is the energy consumption of the chiller, $W \cdot Q$ is the chiller cooling capacity, $W \cdot T_{cws}$ is the supply temperature of cooling water, $°C \cdot T_{chws}$ is the supply temperature of chilled water, $°C \cdot a_1$, b_1, c_1, d_1, e_1, f_1 is the model parameters of chiller.

3.2 Refrigeration Water Pump Energy Consumption Modeling. The chilled water pump delivers chilled water to the air-conditioning end equipment to provide cooling capacity for the air-conditioning end equipment. The flowrate of chilled water affects

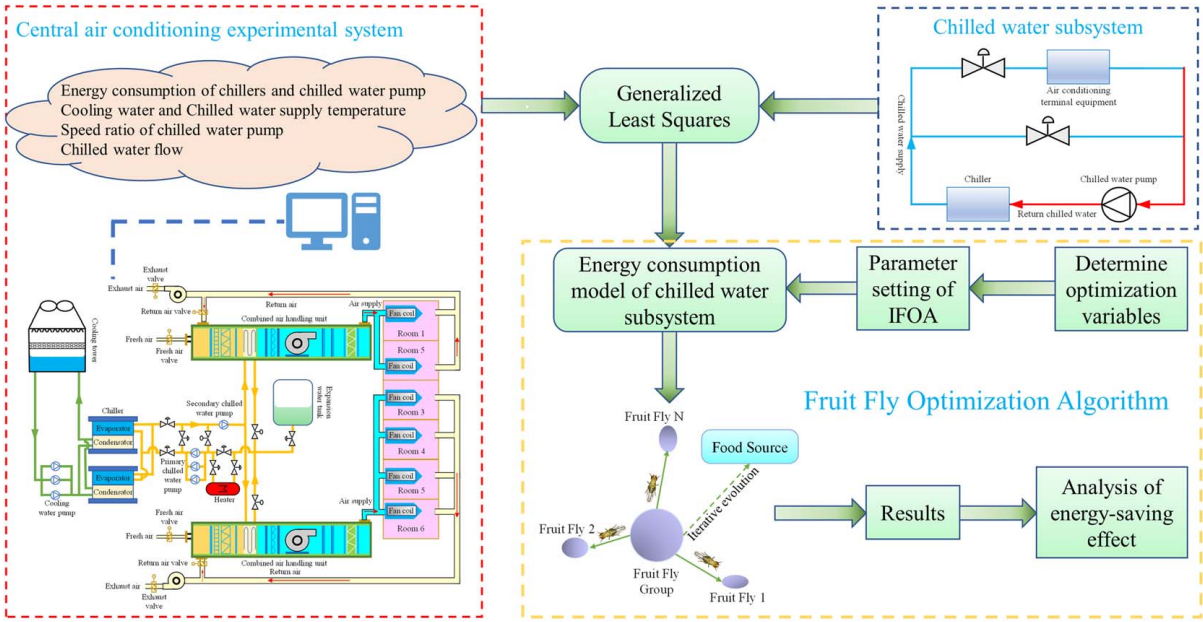

Fig. 2 Research framework

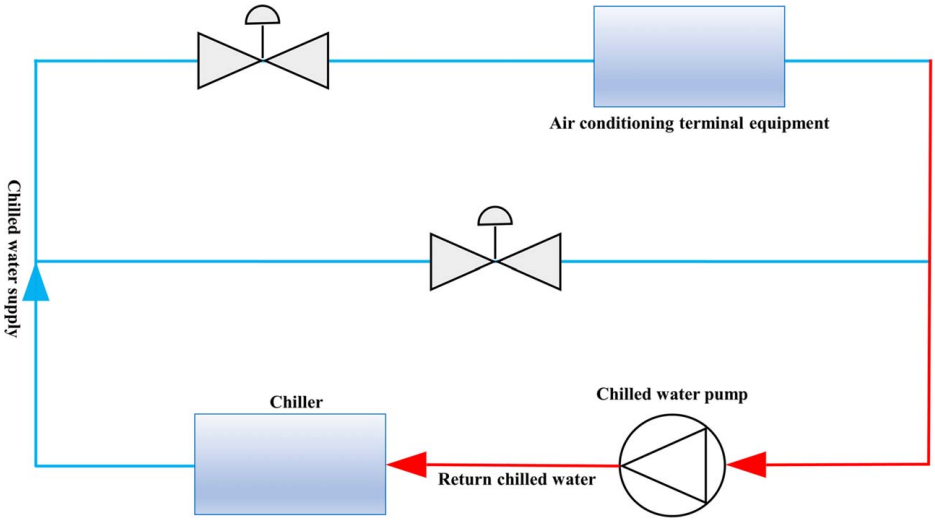

Fig. 3 Chilled water circulation system

the cooling capacity, if the chilled water flowrate is too small, it cannot meet the load requirements of the air-conditioning end; if the chilled water flowrate is too large, the energy consumption of the chilled water pump increases, resulting in energy waste. According to the chilled water pump energy consumption model proposed by ASHRAE Handbook [26], the energy consumption of a chilled water pump is related to the flowrate of chilled water, the head of the pump, and the pump efficiency. The energy consumption model of a chilled water pump can be expressed as

$$P_{pump} = a_2 {r_{chw}}^2 + b_2 r_{chw} \cdot m_{chw} + c_2 {m_{chw}}^2 + \frac{d_2}{r_{chw}} \cdot {m_{chw}}^3 \quad (2)$$

where P_{pump} is the energy consumption of the chilled water pump, $W \cdot m_{chw}$ is the actual flowrate of the chilled water pump, $m^3/h \cdot r_{chw}$ is the chilled water pump speed ratio. a_2, b_2, c_2, d_2 is the model parameters of the chiller pump.

3.3 Chilled Water Subsystem Energy Consumption Modeling. The equipment optimization problem of the chilled water system can be described as adjusting the operating parameters of each piece of equipment to minimize the total energy consumption of the system equipment under the condition of meeting the load demand. The decision variables of the central air-conditioning chilled water system need to meet the requirements of easy adjustment and high correlation with the energy consumption of the system equipment, so the chilled water supply temperature and the speed ratio of the chilled water pump are selected as the optimization variables in this paper. In order to ensure that the chilled water system can operate safely and stably, and to calculate the combination of parameters that meet the actual operation rules, the optimization problem should satisfy the following constraints. Among them, the inequality constraint includes chilled water supply temperature constraint, chilled water pump speed constraint, and the equation constraint is mainly the energy balance relationship inside the chiller unit. In summary, the energy consumption model of the central air-conditioning chilled water system is

$$\begin{aligned} &\min(P) \rightarrow optimal(Tchws, r_{chw}) \\ &P = P_{chiller} + P_{pump} \\ &\begin{cases} T_{chws\min} \le Tchws \le T_{chws\max} \\ 0 \le r_{chw} \le 1 \\ Q = m_{chw} \cdot c_{water} \cdot (T_{cws} - T_{chws}) \end{cases} \end{aligned} \quad (3)$$

where P is the energy consumption of the chilled water system, $W \cdot c_{water}$ is the specific heat capacity of water, 4.18 kJ/kg $m^3 \cdot T_{chws\min}$ is the lower limit of chilled water supply temperature. $T_{chws\max}$ is the upper limit of chilled water supply temperature.

4 Improved Fruit Fly Optimization Algorithm

4.1 Basic Fruit Fly Optimization Algorithm. The fruit fly is widely found in the temperate tropics around the world. Compared with other organisms, the fruit fly has a more developed sense of smell and vision. They rely on their acute sense of smell to find the location of food, share it with other individuals or receive information from other individuals to obtain the location of the individual with the best smell, and use their developed vision to fly to that location to form the center of a new group of fruit fly, and so on until they find food. The process of fruit flies searching for food is shown in Fig. 4.

Based on the characteristics of the fruit fly population foraging behavior, Dr. Wenchao Pan from Taiwan, China proposed a novel bionic-like meta-heuristic intelligent optimization algorithm, the fruit fly optimization algorithm (FOA), in 2012 [18]. The standard FOA is divided into two parts, olfactory search and visual search, and its general steps are as follows:

Step 1: Initialize the fruit fly population. Given the fruit fly population size (*Sizepop*), the maximum number of iterations (*Maxgen*), and the search step (R), randomly initialize the fruit fly population locations X_axis, Y_axis.

Step 2: Fruit fly individuals perform the olfactory search. Each fruit fly individual is given a random search direction and searches distance by Eq. (4)

$$\begin{cases} X_i = X\_axis + RandomValue \\ Y_i = Y\_axis + RandomValue \end{cases} \quad (4)$$

Step 3: Since the food location is unknown, the distance (*Dist*) between the individual fruit fly and the coordinate origin is

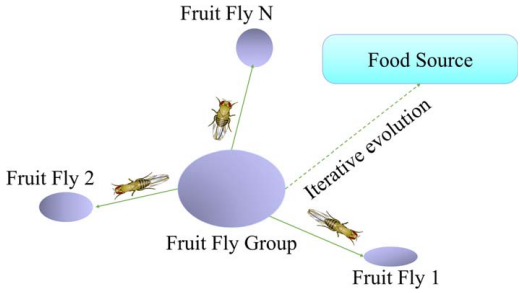

Fig. 4 Search for food by Fruit fly populations

first calculated by Eq. (5), and then the smell concentration judgment value (S) is calculated by Eq. (6)

$$Dist_i = \sqrt{(X_i^2 + Y_i^2)} \tag{5}$$

$$S_i = 1/Dist_i \tag{6}$$

Step 4: Bring the smell concentration judgment value (S) into the smell concentration determination function (fitness function), and calculate the smell concentration (*Smell*) for individual fruit fly by Eq. (7)

$$Smell_i = Function(S)_i \tag{7}$$

Step 5: Identify the individual with the best flavor concentration value within the fruit fly population

$$[bestSmell, bestIndex] = \min(Smell) \tag{8}$$

Step 6: The optimal flavor concentration value and its location information are retained, and the other individuals within the population fly toward the location by visual search

$$\begin{cases} Smellbest = bestSmell \\ X\_axis = X(bestIndex) \\ Y\_axis = Y(bestIndex) \end{cases} \tag{9}$$

Step 7: Enter the iterative optimization search, repeat Steps 2 to 5, and determine whether the optimal flavor concentration value of the contemporary generation is better than that of the previous generation, if yes, then execute Step 6.

The flowchart of the fruit fly optimization algorithm is shown in Fig. 5.

4.2 Improved Fruit Fly Optimization Algorithm. Wu et al. [27] compared the optimization performance of FOA with the ant colony algorithm (ACO), artificial fish swarm algorithm (AFSA), immune algorithm (IA), genetic algorithm (GA), and particle swarm optimization (PSO), and the results are shown in Table 1. From Table 1, it can be seen that FOA is less computationally intensive and has a shorter running time, higher convergence accuracy, faster convergence, and strong global optimization-seeking capability compared to other optimization algorithms.

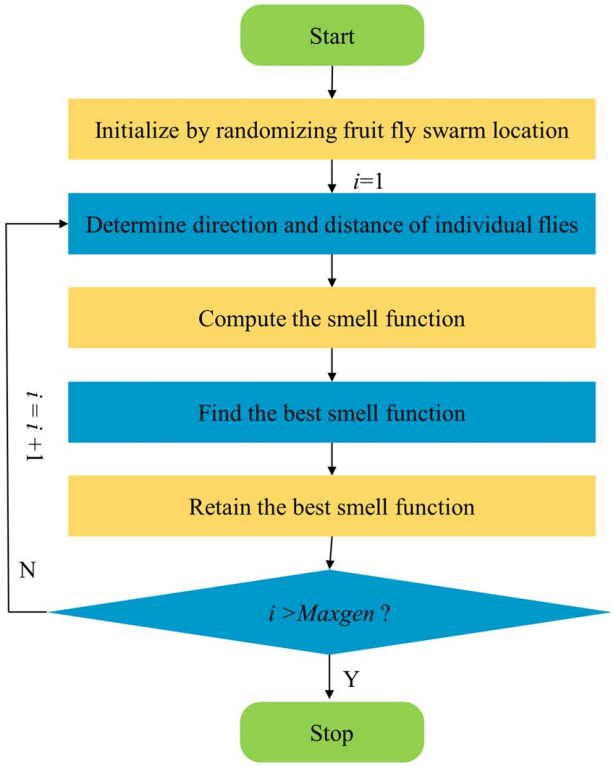

Fig. 5 Standard FOA schematic flowchart

Although FOA has many advantages, it still has some drawbacks:

(1) The initial positions of fruit fly populations are generated randomly, and this randomness can produce improper selection, which leads to slow convergence and a tendency to fall into local optima.
(2) In the basic FOA, the search step is a fixed value, and if the search step is small, it will lead to slow convergence and easy to fall into local optimum; on the contrary, a larger search step, strong oscillation in the late iteration and reduced local search ability.
(3) According to Table 1, it can be seen that the FOA is not very stable.

Based on the above problems, this paper introduces 3-D position coordinates, Arnold Cat Map and variable-step size strategy to improve FOA, and proposes an improved fruit fly optimization algorithm (IFOA) to improve the local search ability and the ability to jump out of the local optimum of FOA.

4.2.1 Three-Dimensional Coordinates. In real life, fruit fly individuals move in 3-D space, and they usually have a large search space to find food easily; however, the fruit fly individuals in FOA search in 2-D space, which reduces the search space of the fruit fly population. Therefore, Pan et al. [28] extended the coordinates of fruit fly individuals into 3-D space, and the location coordinates of the fruit fly population in 3-D became *X_axis*, *Y_axis* and *Z_axis*. The formula for determining the smell concentration judgment value (S) in IFOA became

$$Dist_i = \sqrt{(X_i^2 + Y_i^2 + Z_i^2)} \tag{10}$$

$$S_i = 1/Dist_i \tag{11}$$

4.2.2 Chaotic Mapping. When performing the initialization of the algorithm, the initial positions of the fruit fly population are generated randomly, and this randomness often produces improper selection, which leads the algorithm to fall into the local optimum easily. In order to improve the solution accuracy and convergence speed of the algorithm, this paper introduces chaotic mapping to improve the performance of the algorithm by generating an initial population that can be uniformly spread across the solution space with the help of the randomness and ergodicity of chaotic mapping.

Arnold Cat Map is a discrete chaotic model proposed by the Russian mathematician Vladimir, so named because of the frequent use of a cat face demonstration [29]. Its 2-D mapping form can be expressed as

$$\begin{bmatrix} x_{n+1} \\ y_{n+1} \end{bmatrix} = \begin{bmatrix} 1 & 1 \\ 1 & 2 \end{bmatrix} \begin{bmatrix} x_n \\ y_n \end{bmatrix} \bmod 1 \tag{12}$$

Defining the matrix $C = \begin{bmatrix} 1 & 1 \\ 1 & 2 \end{bmatrix}$, the determinant C has a value of 1. This method can generate points with nonoverlapping, uniform distribution, and good diversity, and the distribution of generated points in 2-D space is shown in Fig. 6.

Extending the 2-D Arnold Cat Map to 3-D by introducing two control parameters u and v, the 2-D mapping can be expressed as

$$\begin{bmatrix} x_{n+1} \\ y_{n+1} \end{bmatrix} = \begin{bmatrix} 1 & u \\ v & uv+1 \end{bmatrix} \begin{bmatrix} x_n \\ y_n \end{bmatrix} \bmod 1 \tag{13}$$

Extending the mapping to the 3-D plane and making 2-D mappings in the x–y, y–z, and x–z planes in turn, and connecting the equations yields

$$\begin{bmatrix} x_{n+1} \\ y_{n+1} \\ z_{n+1} \end{bmatrix} = A \begin{bmatrix} x_n \\ y_n \\ z_n \end{bmatrix} \bmod 1 \tag{14}$$

Table 1 Performance comparison of different optimization algorithms

Algorithm	Performance					
	Complexity	Astringency	Calculation volume	Global optimization search	Local advantage search	Stability
FOA	Simple	Precocious	Smaller	Very strong	Weaker	Unstable
ACO	More complex	Not easy for precocious	Moderate	Stronger	Stronger	More stable
AFSA	More complex	Not easy for precocious	Larger	Stronger	Moderate	More stable
IA	Very complex	Not easy for precocious	Very large	Very strong	Very strong	Very stable
GA	Very complex	Precocious	Larger	Very strong	Weaker	More stable
PSO	Simple	Not easy for precocious	Moderate	Stronger	Moderate	Unstable

In the formula

$$A=\begin{bmatrix}1 & u_z & 0\\ v_z & u_zv_z+1 & 0\\ 0 & 0 & 1\end{bmatrix}\cdot\begin{bmatrix}1 & 0 & 0\\ 0 & 1 & u_x\\ 0 & v_x & u_xv_x+1\end{bmatrix}\cdot\begin{bmatrix}1 & 0 & 0\\ 0 & 1 & u_y\\ v_y & 0 & u_yv_y+1\end{bmatrix} \tag{15}$$

where u_x, u_y, u_z, v_x, v_y, v_z are integers, when $u_x=u_y=u_z=v_x=v_y=v_z=1$, $A=\begin{bmatrix}2 & 1 & 3\\ 3 & 2 & 5\\ 2 & 1 & 4\end{bmatrix}$, the expression of the 3-D Arnold transformation is

$$\begin{bmatrix}x_{n+1}\\ y_{n+1}\\ z_{n+1}\end{bmatrix}=\begin{bmatrix}2 & 1 & 3\\ 3 & 2 & 5\\ 2 & 1 & 4\end{bmatrix}\begin{bmatrix}x_n\\ y_n\\ z_n\end{bmatrix}\bmod 1 \tag{16}$$

4.2.3 Dynamic Step Strategy. In FOA, fruit fly individuals move around according to a fixed step size each time, and the size of the fixed step size will directly affect the performance of individuals in acquiring target source accuracy. If the step size is set too large, the algorithm will speed up the global exploration and improve the convergence speed at the early stage of the iterative search, but when the algorithm enters the late stage of the iterative search, it needs to conduct a fine search in the local area to improve the convergence accuracy, and an overly large step size will miss the global optimum or fall into the local optimum. If the step size is set too small, although it can improve the search accuracy in the late stage of the algorithm, it cannot provide faster search speed in the early iteration. Therefore, the dynamic variable-step size strategy is proposed in this paper.

The rate of change of the concentration difference (Rate) was introduced as the basis for determining the step of change. The rate of change of concentration difference was obtained by comparing the difference between the best and worst concentration values of the fruit fly population during the iterative process with that of the previous generation population, and the formula was calculated as

$$Rate=\left|\frac{best(Smell_i)-worst(Smell_i)}{best(Smell_{i-1})-worst(Smell_i-1)+\lambda}\right| \tag{17}$$

where λ is a smaller positive number used to regulate the denominator to avoid a denominator of 0.

A larger search step should be used to speed up the global search when it is in the early iteration, and a smaller search step should be used to refine the local search when it is in the late iteration. When the rate of change of concentration difference is outside the stable change interval, increase the search step size to speed up the global search rate. When the rate of change of concentration difference is in the stable change interval, it means that the fruit fly population enters the late iteration and starts to fine search, so it is necessary to reduce the search step appropriately. The formula for the change of step length of individual fruit flies is shown in Eq. (18)

$$\begin{cases}R_{gen}=R_{gen-1}-\dfrac{R_{gen-1}\left(\arctan\left(20\cdot\dfrac{gen}{Maxgen}-p\right)+\arctan(q)\right)}{\arctan(20-q)+\arctan(q)}, & Rate\in[\alpha,\beta]\\ R_{gen}=R_{gen-1}+\dfrac{R_{gen-1}\left(\arctan\left(20\cdot\dfrac{gen}{Maxgen}-p\right)+\arctan(q)\right)}{\arctan(20-q)+\arctan(q)}, & Rate\notin[\alpha,\beta]\end{cases} \tag{18}$$

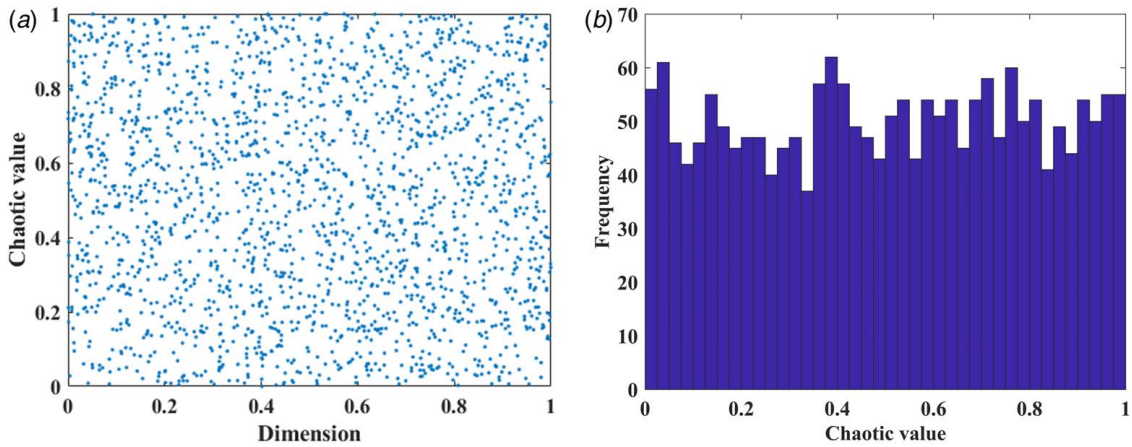

Fig. 6 Arnold Cat Map: (*a*) Arnold Cat Map distribution and (*b*) Arnold Cat Map frequency distribution

where α and β are the boundary values of the stable change interval. R is the population search step. *gen* is the current iteration number. *Maxgen* is the maximum iteration number. q and p are the adjustment coefficients to control the decay of the curve.

Based on the new step update strategy, the step change curves of individual Drosophila are shown in Fig. 7 (with the decreasing step stage). According to Eq. (18), it can be seen that the values of the regulation coefficients p and q affect the decay rate of the curve. In order to obtain a better decay effect, we compared several different combinations of the values of p and q. The results show that the curve can achieve the best decay effect when $p = 8$ and $q = 6$. Based on the new step update strategy, the step change curves of Drosophila individuals are shown in Fig. 7 (taking the step-decreasing stage as an example). According to Eq. (18), it can be seen that the values of regulation coefficients p and q affect the decay rate of the curve. In order to obtain a better decay effect, we compared several different combinations of the values of p and q. The results showed that the curve could achieve the best decay effect when $p = 8$ and $q = 6$.

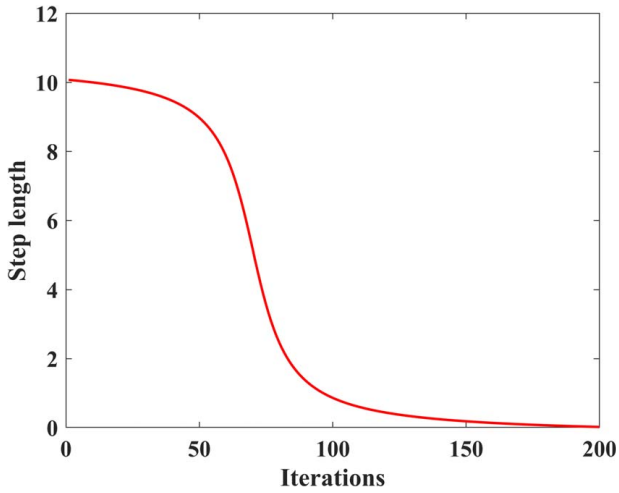

Fig. 7 Step length change curve

4.2.4 Think Beyond the Local Optimum. The above improvements improve the search speed and the search accuracy of the algorithm and reduce the probability of falling into a local optimum, but it still cannot avoid it from falling into a local optimum. Therefore, Arnold Cat Map is introduced again to help the algorithm escape from the local optimum. Set a threshold value δ, and judge whether the algorithm falls into the local optimum based on the size relationship between the variance value σ^2 and δ the test concentration of the fruit fly population. The smaller δ, the denser the population distribution is, the lower the population diversity is, indicating that the algorithm may fall into the local optimum at this time. The calculation formula for σ^2 is shown in Eq. (19)

$$\sigma^2 = \sum_{i=1}^{Sizepop} \left(Smell_i - \left(\sum_{i=1}^{Sizepop} Smell_i / Sizepop \right) \right)^2 \Big/ Sizepop \quad (19)$$

When $\sigma^2 \le \delta$, it is concluded that the algorithm falls into a local optimum, and then the update strategy for the next iteration is changed so that all individuals no longer search around the optimal position, but choose to update the individual positions according to the Arnold Cat Map operation to jump out of the local optimum. The position update formula for fruit fly individuals

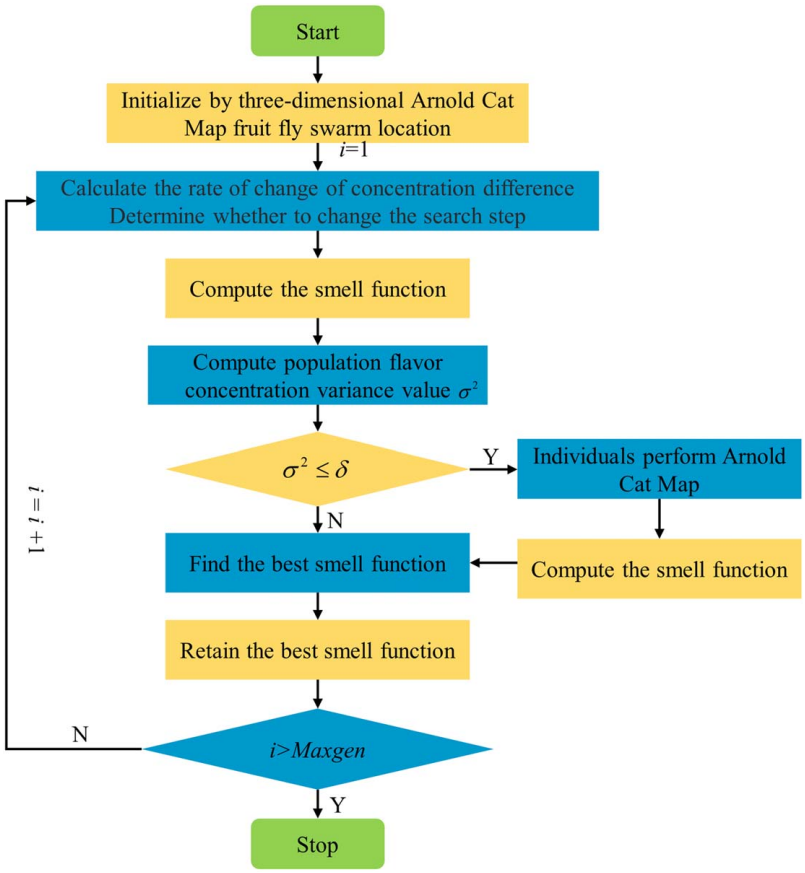

Fig. 8 IFOA flowchart

Table 2 Chilled water system equipment performance parameters

Chillers		Chilled water pump	
Parameters	Numerical value	Parameters	Numerical value
a_1	3.9973	a_2	0.4207
b_1	−2.1201	b_2	1.7010
c_1	0.4953	c_2	−7.2529
d_1	0.0647	d_2	9.1720
e_1	0.0011		
f_1	−0.041		

to jump out of the local optimum is shown in Eq. (20)

$$\begin{cases} X_i = X_i + CAT \\ Y_i = Y_i + CAT \\ Z_i = Z_i + CAT \end{cases} \tag{20}$$

where CAT is a cat mapping of the position coordinates of the individual fruit flies.

4.2.5 IFOA Steps. The steps of IFOA are as follows:

Step 1: Initialize the fruit fly population. Given the population size (*Sizepop*), the maximum number of iterations (*Maxgen*), and the 3-D location coordinates of the initialized individuals by cat mapping *X_axis*, *Y_axis*, *Z_axis*.

Step 2: Obtain the smell concentration judgment value (S) by Eqs. (10) and (11), and calculate the individual smell concentration (*Smell*).

Step 3: Calculate the smell concentration variance of the fruit fly population σ^2 from Eq. (19) and determine whether the population is trapped in a local optimum. If the population is trapped in the local optimum, Arnold Cat Map is performed according to Eq. (20) to jump out of the local optimum and calculate the individual smell concentration (*Smell*).

Step 4: Find the individual with the minimum smell concentration in the fruit fly population.

Step 5: The optimal flavor concentration value and its location information are retained, and the other individuals within the population fly toward the location by visual search.

Step 6: Enter the iterative search for superiority and repeat Steps 2 ~4. The search steps of individual fruit flies are determined by Eqs. (17) and (18), and determine whether the optimal flavor concentration value of the current generation is better than that of the previous generation and if so, perform Step 5.

The flowchart of IFOA is shown in Fig. 8.

5 Case Optimization Results and Analysis

5.1 Optimization Case. The cooling source of the experimental equipment of the central air-conditioning system mentioned in this paper is a rotor compressor with a cooling capacity of 5400 W, which has a rated power of 1700 W and a COP of 3.16. The chilled water and cooling water pumps are each equipped with a variable frequency pump with a rated power of 550 W and a rated flowrate of 5. And a cross-flow cooling tower with a rated power of 180 W is equipped.

5.2 Energy Consumption Model Parameter Identification. Due to the long-term operation of the system, resulting in the actual characteristics of the system equipment is not the same as the factory, therefore, through the collected data of this equipment chiller energy consumption, chilled water supply temperature, cooling water supply temperature, chilled water pump speed ratio, chilled water flowrate, chilled water pump energy consumption, etc., the least squares method is used to identify the parameters of the central air-conditioning chilled water system energy consumption model established in Sec. 3, and the identified performance parameters are shown in Table 2.

In order to verify the accuracy of the chilled water system equipment energy consumption model obtained by identification, 30 different sets of operating data were selected from the collected system operating data, and the energy consumption of the system under each working condition was calculated using the model and compared with the actual energy consumption of the equipment, and the actual and calculated energy consumption scatter diagrams of chilled water pumps and chillers were drawn as shown in Fig. 9, and the performance indexes of the model were also calculated as shown in Table 3, from which it can be seen that R^2 of chiller and chilled water pump are 0.9451 and 0.9279 respectively, which are close to 1. Therefore, the energy consumption model can be used for energy-saving optimization of the chilled water system.

5.3 Simulation Results. In this section, 30 sets of actual working conditions are selected and optimized by simulation using MATLAB 2017A. The actual load demand corresponding to each working condition is shown in Table 4. It can be seen that

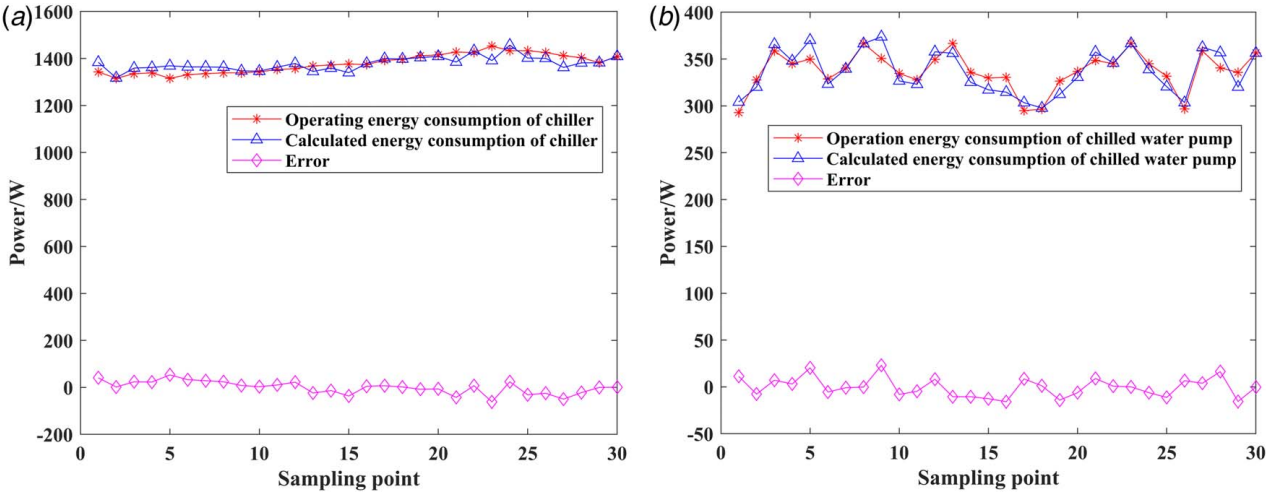

Fig. 9 Comparison of actual and calculated energy consumption of equipment: (*a*) chiller and (*b*) chilled water pump

Table 3 Performance indicators for identification of equipment parameters

Equipment	MAE	MSE	RMSE	R^2
Chillers	21.3	7.2758e−01	27	0.9451
Chilled water pump	8.3	1.0416e−01	2	0.9279

Table 4 Optimized parameter settings for IFOA

Parameters	Numerical value	Parameters	Numerical value
T_{chwr}	15 °C	β	1.05
T_{cws}	32 °C	R	1
$T_{chwsmin}$	5 °C	q	6
$T_{chwsmax}$	15 °C	z	8
Sizepop	100	δ	10e−05
Maxgen	300	σ^2	0.01
α	0.95		

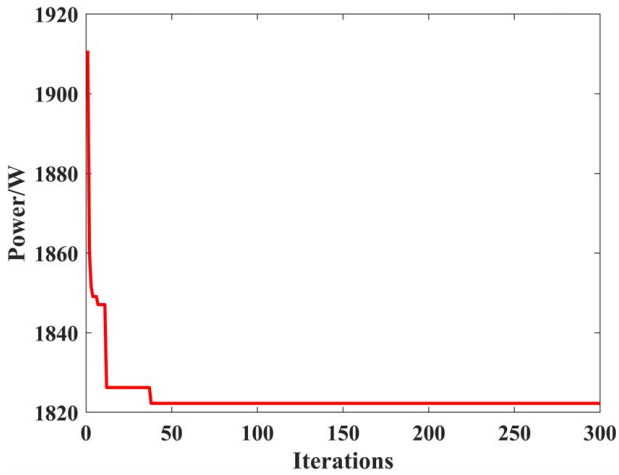

Fig. 10 Minimum consumption iteration curve for $Q = 4000$ W

the system load changes within the design load, and if various equipment cannot be dynamically adjusted with the change in load demand, it will lead to inefficient equipment operation Therefore, it is very necessary to optimize the operating parameters of the system equipment Considering that the control variables need to satisfy easy adjustment and high correlation with chilled water system equipment energy consumption, the chilled water supply temperature and the speed ratio of chilled water pump are used as the optimized control variables for this optimization problem in this paper. The parameter settings for the energy-saving optimization of the central air-conditioning chilled water system based on IFOA are shown in Table 4 [25].

Figure 10 shows the convergence curve of system energy consumption in the process of optimizing the operating parameters of the chilled water system using IFOA with the chiller's cooling capacity of 4000 W as an example. As can be seen from Fig. 10, the optimization of the chilled water system energy consumption

Table 5 Comparison of energy consumption before and after optimization of 30 sampling points

Sampling points	Cold load (W)	Actual power (W)	Optimized power (W)	Parameters		Energy saving (W)
				T_{chws} (°C)	r_{chw}	
1	3240.7	1635.8	1580.7	5.92	0.72	55.14
2	3178.5	1643.2	1574.8	6.28	0.7	68.48
3	2861.3	1693.7	1608.7	5.9	0.7	85.05
4	2947.1	1683.7	1589.7	5.93	0.8	94.01
5	3206.6	1665.3	1582.4	7.75	0.76	82.95
6	2960.8	1659.9	1588.7	5.14	0.7	71.21
7	3015.2	1675.4	1580.5	6.48	0.73	94.99
8	3024	1705.3	1579	5.32	0.73	126.34
9	3037.8	1689.7	1579.1	6.82	0.71	110.66
10	3045.9	1677.6	1576.6	5.37	0.72	101.09
11	3092.1	1680.5	1575.7	5.84	0.79	104.8
12	3097.1	1705.97	1576.2	5.34	0.73	129.77
13	3103.1	1735	1574.7	5.58	0.73	160.34
14	3103.6	1708	1574.6	6.23	0.81	133.49
15	3103.6	1706	1575.6	5.30	0.75	130.43
16	3112.5	1704.4	1575.4	6.75	0.75	129.09
17	3118.5	1686.8	1574.3	6.04	0.74	112.54
18	3122.8	1692.4	1574.6	5.63	0.71	117.83
19	3130.6	1738	1573.2	5.00	0.7	164.88
20	3162.5	1751.9	1575.3	5.90	0.7	176.62
21	3168.5	1775.8	1574.5	5.56	0.72	201.36
22	3176.6	1770.2	1575.8	5.05	0.75	194.49
23	3207.5	1819.3	1579.9	5.19	0.78	239.49
24	3166.3	1777.8	1573.9	5.02	0.7	203.92
25	3153.1	1764.8	1575.1	5.00	0.73	189.75
26	3026.6	1722.1	1579.1	5.45	0.71	143.09
27	2861.3	1770.2	1608.7	5.11	0.73	161.51
28	2947.1	1744	1590.4	6.25	0.71	153.63
29	2960.8	1717.5	1588.1	5.25	0.86	129.46
30	3026.6	1764.5	1578.4	5.29	0.7	186.17

Table 6 Energy consumption and parameter settings for each system at different cooling capacities

	IFOA			FOA			PSO			SCA		
Chiller load	Power (W)	Parameter	Value	Power (W)	Parameter	Value	Power (W)	Parameter	Value	Power (W)	Parameter	Value
40%	1768.3	T_{chws}	11.27	1769.7	T_{chws}	11.71	1770.8	T_{chws}	11.90	2071.6	T_{chws}	11.89
		r_{chw}	0.73		r_{chw}	0.72		r_{chw}	0.75		r_{chw}	0.8
50%	1531.1	T_{chws}	6.44	1533.5	T_{chws}	8.4	1533.9	T_{chws}	8.19	1753.7	T_{chws}	5.31
		r_{chw}	0.73		r_{chw}	0.71		r_{chw}	0.82		r_{chw}	0.75
60%	1455	T_{chws}	5.29	1456.7	T_{chws}	5.65	1456.4	T_{chws}	5.14	1689.8	T_{chws}	5.01
		r_{chw}	0.74		r_{chw}	0.71		r_{chw}	0.77		r_{chw}	0.75
70%	1656.7	T_{chws}	5.43	1660.1	T_{chws}	5.99	1659.2	T_{chws}	5.11	1903.4	T_{chws}	5.02
		r_{chw}	0.75		r_{chw}	0.75		r_{chw}	0.72		r_{chw}	0.77
80%	2146.9	T_{chws}	5.31	2150.6	T_{chws}	6.41	2149.9	T_{chws}	5.17	2405.3	T_{chws}	5.43
		r_{chw}	0.75		r_{chw}	0.84		r_{chw}	0.75		r_{chw}	0.80
90%	2925.4	T_{chws}	5.19	2929.2	T_{chws}	5.51	2928.9	T_{chws}	5.04	3189.1	T_{chws}	5.22
		r_{chw}	0.76		r_{chw}	0.71		r_{chw}	0.78		r_{chw}	0.83

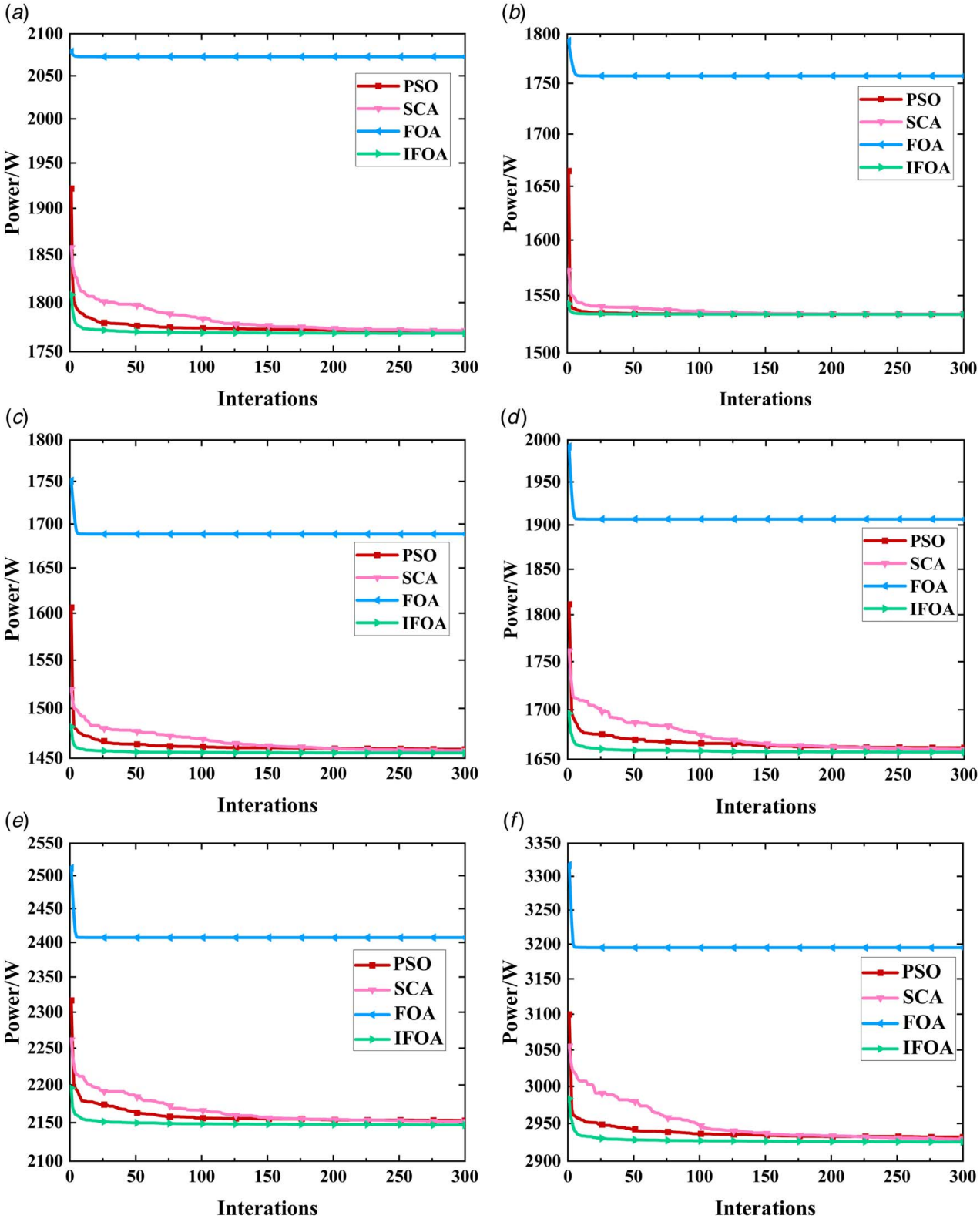

Fig. 11 Iteration curve of each algorithm under different loads: (*a*) 40% load rate, (*b*) 50% load rate, (*c*) 60% load rate, (*d*) 70% load rate, (*e*) 80% load rate, and (*f*) 90% load rate

by IFOA has a fast speed, and the lowest value of the chilled water system operating energy consumption is obtained when the number of iterations reaches about 40, at which the lowest value of the chilled water system operating energy consumption is 1822.4 W. The corresponding parameter values include $T_{chws} = 5.56$, $r_{chw} = 0.71$.

The optimization results for 30 sets of working conditions are shown in Table 5. In order to better analyze the optimization effect, the overall energy consumption before and after the optimization of these 30 groups of actual working conditions was compared. As shown in Table 5, the optimized energy consumption in all 30 groups of conditions was significantly reduced, and the

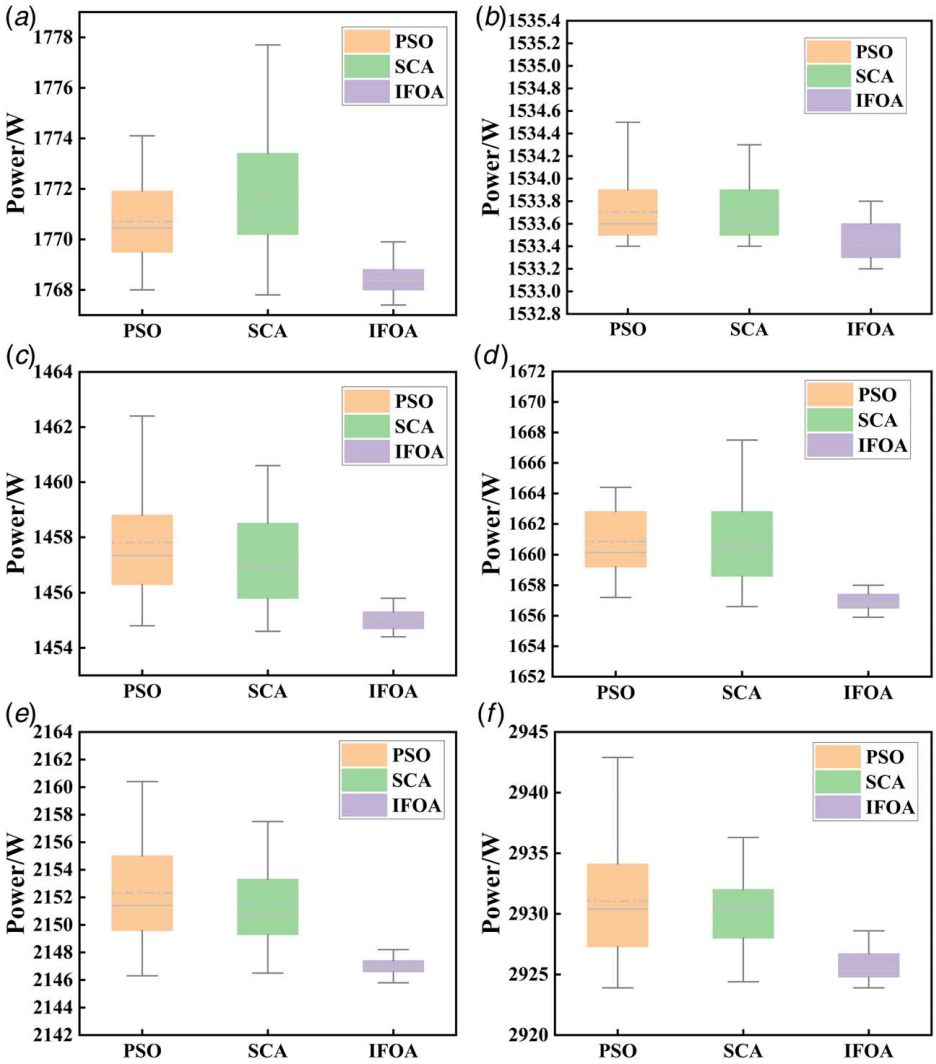

Fig. 12 Result distribution of 30 independent runs of PSO, SCA, and IFOA under different loads: (*a*) 40% load rate, (*b*) 50% load rate, (*c*) 60% load rate, (*d*) 70% load rate, (*e*) 80% load rate, and (*f*) 90% load rate

calculated energy consumption of the optimized chilled water system was 7.9% on average compared with that before optimization.

5.4 Experimental Platform Verification. From Sec. 5.3, it can be seen that the energy-saving effect of the IFOA-based chilled water system optimization method is obvious, but the above experimental results are based on computer simulations, which is not very comprehensive to judge the application effect of the method in the actual system. In order to further verify the performance of the IFOA algorithm in the actual system, experiments were conducted on the experimental platform of the central air-conditioning system mentioned in Sec. 2. Six typical operating conditions of 40%, 50%, 60%, 70%, 80%, and 90% of the system design load were selected to analyze the actual performance of IFOA in three aspects: actual optimization results, convergence and robustness, and to compare with particle swarm optimization algorithm (PSO) [30], the sine cosine optimization algorithm (SCA) [31] and FOA. To ensure the fairness of the comparison results, the common parameters (population size, maximum number of iterations, etc.) of each algorithm are kept consistent. Experimental platform verification.

5.5 Analysis of Experimental Results. First, this experimental platform combines PSO, SCA, and FOA algorithms to obtain optimized operating parameters and optimization results as shown in Table 6, compared with PSO, SCA, and FOA, IFOA algorithm has a better energy-saving effect.

Since IFOA is improved on the basis of FOA algorithm, in order to better compare and verify the optimization effect of IFOA algorithm for actual chilled water system, in addition to PSO and SCA algorithms, the comparison analysis with FOA algorithm was added from two aspects of convergence and robustness. From the convergence curves of the four algorithms under six load rate conditions in Fig. 11, it can be seen that IFOA can optimize the system faster than the other three algorithms. Therefore, the IFOA algorithm has better convergence in practical applications.

Finally, the maximum, minimum, and average values of the optimization results are shown in Fig. 12 for 30 independent experiments using the four algorithms for the above six conditions. The maximum, minimum, and average values of the optimization results obtained by IFOA are better than those of PSO, SCA, and FOA. Meanwhile, the difference between the maximum and minimum values obtained by the IFOA algorithm is the smallest among the four algorithms. Therefore, the IFOA algorithm has good robustness.

6 Conclusion

This paper establishes an energy consumption model for the energy-using equipment of the chilled water subsystem of central air conditioning and uses the least squares method to identify it

and obtain the model parameters of the chilled water subsystem. Since the traditional FOA is easy to fall into local optimum and is not very stable, an improved fruit fly optimization algorithm is proposed in this paper to improve the performance of FOA. The main improvements to the FOA are as follows.

(1) Expanding the 2-D position coordinates of individual fruit flies to 3-D space increases the search space of the fruit fly population.
(2) Introduce cat mapping to generate the initial population of the fruit fly population to reduce the effect of uneven distribution of the initial population and improve the convergence speed of the algorithm.
(3) Establish a dynamic search step update strategy to balance the global search capability and local search capability of the algorithm.
(4) Calculate the value of the flavor concentration variance of the fruit fly population, determine whether the population is trapped in a local optimum, and help the individuals trapped in a local optimum to jump out with Arnold Cat Map.

The energy-saving optimization of a central air-conditioning chilled water system was performed in MATLAB 2017A using the IFOA algorithm. The results show that the optimization of the operating parameters of the chilled water system using IFOA can reduce the operating energy consumption of the system with an energy-saving rate of 7.9%. In addition, the optimization capability, convergence, and robustness of IFOA are verified by comparing it with FOA, PSO, and SCA algorithms for different working conditions. The results show that the IFOA-based chilled water energy efficiency optimization method can provide a feasible approach for the energy efficiency optimization of central air-conditioning systems.

In this paper, the chilled water system of a central air-conditioning system is studied for energy-saving optimization, but there are some shortcomings due to the limitation of research conditions and other factors.

(1) This paper is based on the previous simplified water system equipment energy consumption model, and the equipment energy consumption mathematical model still has some errors. In the future scientific research and practice, it is necessary to further deepen the improvement, in order to establish a closer to the actual situation of the equipment energy consumption mathematical model.
(2) We only studied the chilled water system alone, while the whole air-conditioning system consists of chilled water system, cooling water system, and air system together. Therefore, to achieve better energy savings, the entire air-conditioning system needs to be added to the optimization model.
(3) The central air-conditioning system we studied is based on one experimental equipment in the laboratory, and due to some constraints, the scale of this group of experimental equipment is relatively small, and the parallel operation of the chiller and other equipment cannot be studied. In subsequent studies, we can consider larger-scale central air-conditioning systems and include the start/stop and number of units control of energy-consuming equipment in the optimization variables, making the optimization model have a wider application range.

Acknowledgment

This work was supported by the Shaanxi Provincial Education Department 2022 Key Research Program Project (22JS022), Natural Science Foundation of China (51808428).

Conflict of Interest

There are no conflicts of interest.

Data Availability Statement

The datasets generated and supporting the findings of this article are obtainable from the corresponding author upon reasonable request.

Nomenclature

Variables

p = curve decay degree adjustment factor
q = curve decay degree adjustment factor
u = control parameter
v = control parameter
x = unknown number
y = unknown number
z = unknown number
P = energy consumption of chilled water system
Q = chiller cooling capacity
R = search step
S = smell concentration judgment value
W = Watt
X = X coordinate of the individual
Y = Y coordinate of the individual
Z = Z coordinate of the individual
c_{water} = specific heat capacity of water
m_{chw} = actual flowrate of the chilled water pump
r_{chw} = chilled water pump speed ratio
$P_{chiller}$ = energy consumption of the chiller
P_{pump} = energy consumption of the chilled water pump
T_{chwr} = return temperature of chilled water
T_{chws} = supply temperature of chilled water
$T_{chws\max}$ = upper limit of chilled water supply temperature
$T_{chws\min}$ = lower limit of chilled water supply temperature
T_{cws} = supply temperature of cooling water
$a_1, b_1, c_1, d_1, e_1, f_1$ = performance parameters of chiller
a_2, b_2, c_2, d_2 = performance parameters of chilled water pump
bestIndex = individual with minimum smell concentration
bestSmell = minimum smell concentration
Dist = the distance between the individual and the coordinate origin
Function = fitness function
gen = current iteration number
Maxgen = maximum number of iterations
RandomValue = random flying distance
Rate = rate of change of concentration difference
Sizepop = fruit fly population size
Smell = smell concentration
Smellbest = historical optimal flavor concentration values
α = the lower boundary of the stable change interval
β = the upper boundary of the stable change interval
δ = current number of iterations
λ = denominator regulator
σ^2 = fruit fly population smell concentration variance value
°C = degree celsius

Abbreviations

ACO = ant colony algorithm
AFSA = artificial fish swarm algorithm
CAT = Arnold Cat Map
FOA = fruit fly optimization algorithm

GA = genetic algorithm
IA = immune algorithm
IFOA = improved fruit fly optimization algorithm
MAE = average absolute error
MSE = mean square error
PCA-ANN = principal component analysis-artificial neural network
PSO = particle swarm optimization
RMSE = root mean square error
R^2 = decision factor

References

[1] National Bureau of Statistics, 2022, "National Data." https://data.stats.gov.cn/easyquery.htm?cn=C01
[2] Xinhua News Agency, 2021, "Opinions on Completely, Accurately and Comprehensively Implementing the New Development Concept and Doing a Good Job of Carbon Peak and Carbon Neutralization." http://www.gov.cn/zhengce/2021-10/24/content_5644613.htm
[3] Ye, Y., Zuo, W., and Wang, G., 2019, "A Comprehensive Review of Energy-Related Data for U.S. Commercial Buildings," Energy Build., **186**, pp. 126–137.
[4] Takabatake, T., Yamamoto, M., and Hino, H., 2021, "Algorithm for Searching Optimal Set Values of Absorption Chiller System Using Bayesian Optimization," Sci. Technol. Built Environ., **28**(2), pp. 188–199.
[5] Zheng, Z.-X., and Li, J.-Q., 2018, "Optimal Chiller Loading by Improved Invasive Weed Optimization Algorithm for Reducing Energy Consumption," Energy Build., **161**, pp. 80–88.
[6] Mu, B., Li, Y., House, J. M., and Salsbury, T. I., 2017, "Real-Time Optimization of a Chilled Water Plant With Parallel Chillers Based on Extremum Seeking Control," Appl. Energy, **208**, pp. 766–781.
[7] Zhou, Y., Li, X., and Yang, D., 2022, "Optimization of Metro Central Air Conditioning Cold Source System Based on PCA-ANN Data Model," Front. Energy Res., **10**, p. 762275.
[8] Yu, F. W., and Chan, K. T., 2008, "Optimization of Water-Cooled Chiller System With Load-Based Speed Control," Appl. Energy, **85**(10), pp. 931–950.
[9] Kelvin Wijaya, T., Sholahudin, Idrus Alhamid, M., Saito, K., and Nasruddin, N., 2022, "Dynamic Optimization of Chilled Water Pump Operation to Reduce HVAC Energy Consumption," Ther. Sci. Eng. Prog., **36**, p. 101512.
[10] Deng, J., He, S., Wei, Q., Liang, M., Hao, Z., and Zhang, H., 2020, "Research on Systematic Optimization Methods for Chilled Water Systems in a High-Rise Office Building," Energy Build., **209**, p. 109695.
[11] Yu, J., Liu, Q., Zhao, A., Chen, S., Gao, Z., Wang, F., and Zhang, R., 2021, "A Distributed Optimization Algorithm for the Dynamic Hydraulic Balance of Chilled Water Pipe Network in Air-Conditioning System," Energy, **223**, p. 120059.
[12] Shi, W., Wang, J., Lyu, Y., Jin, X., and Du, Z., 2021, "Optimal Control of Chilled Water Systems Based on Collaboration of the Equipment's Near-Optimal Performance Maps," Sustain. Energy Technol. Assess., **46**, p. 101236.
[13] Du, J., Li, S., and Li, X., 2021, "Modeling and Optimization of a Chilled-Water Cooling System With Multiple Chillers," Therm. Sci., **25**(5 Part B), pp. 3873–3888.
[14] Kusiak, A., Li, M., and Tang, F., 2010, "Modeling and Optimization of HVAC Energy Consumption," Appl. Energy, **87**(10), pp. 3092–3102.
[15] Jiao, X., and Xu, Q., 2019, "Optimization Analysis on the Effect of Operational Power Consumption for Central Air Conditioning Under Cold Storage Regulation," Int. Trans. Electr. Energy Syst., **29**(5), p. e12001.
[16] Chen, J., He, Z., and Hongfu, Z., 2022, "Energy Consumption Modeling and Optimization of VAV Central Air Conditioning System (in Chinese)," Ship Eng., **44**(01), pp. 27–31+58.
[17] Ma, Z., and Wang, S., 2011, "Supervisory and Optimal Control of Central Chiller Plants Using Simplified Adaptive Models and Genetic Algorithm," Appl. Energy, **88**(1), pp. 198–211.
[18] Pan, W.-T., 2012, "A New Fruit Fly Optimization Algorithm: Taking the Financial Distress Model As an Example," Knowl. Based Syst., **26**, pp. 69–74.
[19] Yang, Y., Chen, H., Li, S., Heidari, A. A., and Wang, M., 2020, "Orthogonal Learning Harmonizing Mutation-Based Fruit Fly-Inspired Optimizers," Appl. Math. Model., **86**, pp. 368–383.
[20] Qi, M.-Y., Li, J.-Q., Han, Y.-Y., and Dong, J.-X., 2020, "Optimal Chiller Loading for Energy Conservation Using an Improved Fruit Fly Optimization Algorithm," Energies, **13**(15), p. 3760.
[21] Guo, C., Shang, W., and Chen, C.-H., 2021, "Tourist Demand Prediction Model Based on Improved Fruit Fly Algorithm," Secur. Commun. Netw., **2021**, pp. 1–11.
[22] Chen, C., 2020, "RWFOA: A Random Walk-Based Fruit Fly Optimization Algorithm," Soft Comput., **24**(16), pp. 12681–12690.
[23] Lin, W.-M., Tu, C.-S., Tsai, M.-T., and Lo, C.-C., 2015, "Optimal Energy Reduction Schedules for Ice Storage Air-Conditioning Systems," Energies, **8**(9), pp. 10504–10521.
[24] Yu, F. W., and Chan, K. T., 2005, "Energy Signatures for Assessing the Energy Performance of Chillers," Energy Build., **37**(7), pp. 739–746.
[25] Chen, L., 2020, "Research on Enery Saving Optimization of Water System of HVAC Based on Genetic Ant Colony Hybrid Algorithm (in Chinese)," Master's Thesis, Shandong University of Science and Technology, Qingdao, China.
[26] Parsons, R., 2000, "ASHARE Research: Improving the Quality of Life," HVAC Systems and Equipment, ASHRAE.
[27] Wu, X., 2013, "Research on the Optimization Performance of Fruit Fly Optimisation Algorithm and Five Species Intelligent Algorithm (in Chinese)," Fire Control Command Control, **38**(04), pp. 17–20+25.
[28] Pan, W.-T., 2013, "Using Modified Fruit Fly Optimisation Algorithm to Perform the Function Test and Case Studies," Conn. Sci., **25**(2–3), pp. 151–160.
[29] AvaroĞLu, E., 2017, "Pseudorandom Number Generator Based on Arnold Cat Map and Statistical Analysis," Turk. J. Electr. Eng. Comput. Sci., **25**(1), pp. 633–643.
[30] Kennedy, J., 1997, "The Particle Swarm Social Adaptation of Knowledge," IEEE 1997 IEEE International Conference on Evolutionary Computation (ICEC '97), Indianapolis, IN, Apr. 13–16, pp. 303–308.
[31] Mirjalili, S., 2016, "SCA: A Sine Cosine Algorithm for Solving Optimization Problems," Knowl. Based Syst., **96**, pp. 120–133.